Inorganic Chemistry
Article

Inorg. Chem. **2010**, *49*, 9641–9648 **9641**
DOI: 10.1021/ic1014253

Magnetic Properties of Largest-Spin Single Molecule Magnets: Mn_{17} Complexes—A Density Functional Theory Approach

Eduard Cremades and Eliseo Ruiz*

Departament de Química Inorgànica and Institut de Recerca de Química Teòrica i Computacional, Universitat de Barcelona, Diagonal 647, 08028 Spain

Received July 17, 2010

The exchange coupling constants of two Mn_{17} complexes have been analyzed; one of them has the second largest ground-state spin value reported up to now, being the largest-spin single-molecule magnet. The two complexes show a two-edge-sharing supertetrahedra structural motif, $Mn^{II}_6Mn^{III}_{11}$, and similar ligands, but they show different total spin values. One of them has the highest possible, $S = 37$, while for the second complex, the S value is lower and equal to 28 ± 1. The calculated J values using DFT methods for both systems indicate the predominance of the ferromagnetic interactions consistent with the $S = 37$ total spin. The analysis of similar Mn_{19} complexes with the two supertetrahedra sharing one vertex gives similar results, pointing out the preponderance of the ferromagnetic couplings.

Introduction

The discovery in 1993 of the first single-molecule magnet (SMM), the well-known Mn_{12} cluster,[1] opened a new investigation line that has been thoroughly studied for a large number of groups, which has focused on the synthesis of polynuclear compounds that could improve the properties of such complexes. SMM complexes show a splitting of the M_s states due to the presence of the zero-field splitting phenomenon (ZFS).[2,3] The energy difference between the highest and the lowest M_s states caused by the loss of degeneracy could be understood as an energy barrier (U_{eff}), whose height is directly related with the square of the total spin (S) of the molecule and its magnetic axial anisotropy (D) that must be overcome in order to change the spin direction (from $+M_s$ to $-M_s$ states). This D value must be negative to have a barrier instead of a single well; the higher the barrier, the more difficult it is to change the spin direction. This property could lead to applications in information systems at molecular level depositing such molecules on a surface,[4] since the direction of the magnetic moment of bulk materials is employed to store information on hard disks and related devices.[5] Otherwise, it is possible to change the sign of the M_s state passing through the energy barrier. This phenomenon is the well-known quantum tunnel effect, and in conjunction with a fast relaxation of the spin, it goes against the ability to store information. However, this quantum effect could have a future application in quantum computation.[6]

The search for SMMs with improved magnetic properties has led to the synthesis of large polynuclear compounds that show large total spins values up to $S = 83/2$.[7] However, these kinds of compounds usually show very low magnetic anisotropy values, giving not so large energy barriers, and even in some cases do not present SMM behavior because of the positive D values. Recently, a family of Mn_6 complexes was synthesized, showing the highest energy barrier, with total spin values in the range between $S = 4$ and $S = 12$,[8−10] but the barriers are not significantly different from that found in the original Mn_{12} complex.

The aim of the present work is to understand the magnetic properties and, consequently, the total spin values of two Mn_{17} complexes that have been recently synthesized showing a two-edge-sharing supertetrahedra $Mn^{II}_4Mn^{III}_6$ structural

*To whom correspondence should be addressed. E-mail: eliseo.ruiz@qi.ub.es.

(1) Sessoli, R.; Gatteschi, D.; Caneschi, A.; Novak, M. A. *Nature* **1993**, *365*, 141.
(2) Gatteschi, D.; Sessoli, R. *Angew. Chem., Int. Ed.* **2003**, *42*, 246.
(3) Gatteschi, D.; Sessoli, R.; Villain, J. *Molecular Nanomagnets*; Oxford University Press: Oxford, U. K., 2006.
(4) Mannini, M.; Pineider, F.; Sainctavit, P.; Danieli, C.; Otero, E.; Sciancalepore, C.; Talarico, A. M.; Arrio, M.-A.; Cornia, A.; Gatteschi, D.; Sessoli, R. *Nat. Mater.* **2009**, *8*, 194.
(5) Rogez, G.; Donnio, B.; Terazzi, E.; Gallani, J.-L.; Kappler, J.-P.; Bucher, J.-P.; Drillon, M. *Adv. Mater.* **2009**, *21*, 4323.
(6) Timco, G. A.; Caretta, S.; Troiani, F.; Tuna, F.; Pritchard, R. J.; McInnes, E. J. L.; Ghirri, A.; Candini, A.; Santini, P.; Amoretti, G.; Affronte, M.; Winpenny, R. E. P. *Nat. Nanotech.* **2009**, *4*, 173.
(7) Ako, A. M.; Hewitt, I. J.; Mereacre, V.; Clérac, R.; Wensdorfer, W.; Anson, C. E.; Powell, A. K. *Angew. Chem., Int. Ed.* **2006**, *45*, 4926.
(8) Milios, C.; Vinslava, A.; Wernsdorfer, W.; Moggach, S.; Parsons, S.; Perlepes, S.; Christou, G.; Brechin, E. *J. Am. Chem. Soc.* **2007**, *129*, 2754.
(9) Milios, C. J.; Inglis, R.; Vinslava, A.; Bagai, R.; Wernsdorfer, W.; Parsons, S.; Perlepes, S. P.; Christou, G.; Brechin, E. K. *J. Am. Chem. Soc.* **2007**, *129*, 12505.
(10) Cremades, E.; Cano, J.; Ruiz, E.; Rajaraman, G.; Milios, C. J.; Brechin, E. K. *Inorg. Chem.* **2009**, *48*, 8012.

Published on Web 09/21/2010

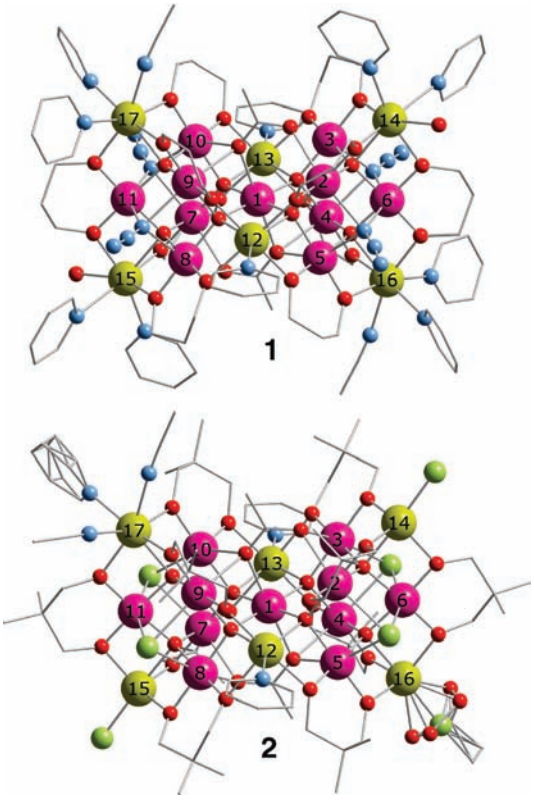

Figure 1. Molecular structures of Mn_{17} complexes, $[Mn^{II}_6Mn^{III}_{11}(\mu_4\text{-}O)_8(\mu_3\text{-}N_3)_4(\mu,\mu_3\text{-}O_2CMe)_2(\mu,\mu\text{-}PD)_{10}(py)_{10}(MeCN)_2(H_2O)_2]^{3+}$ (**1**) and $[Mn^{II}_6Mn^{III}_{11}(\mu_4\text{-}O)_8(\mu_3\text{-}Cl)_4(\mu,\mu_3\text{-}O_2CMe)_2(\mu,\mu\text{-}DPD)_{10}Cl_{2.34}(O_2CMe)_{0.66}(py)_3(MeCN)_2]$ (**2**) (PDH_2 = propanediol; $DPDH_2$ = 2,2-dimethyl-1,3-propanediol; py = pyridine) showing disorder in some external ligands. The Mn^{II} and Mn^{III} cations, oxygen atoms, nitrogen atoms, and chloride atoms are represented as yellow, pink, red, blue, and green spheres, respectively, while hydrogen atoms are omitted for clarity.

motif (see Figure 1).[11,12] Although both compounds have the same metal core, $Mn^{II}_6Mn^{III}_{11}$, and almost identical ligands, they show different total spin values. In complex **1**, this value is the highest possible, $S = 37$, while in the second complex, it is lower and equal to 28 ± 1. Thus, this complex, **1**, has the second largest ground-state spin value reported up to now and is the largest-spin SMM. Also, there are examples in the literature of similar Mn_{17} complexes that can build up 1D or 2D coordination polymers where the clusters are linked by a μ_3-1,3-azide or cianato ligands.[11,13] These two coordination polymers show, at high temperatures, χ_mT values consistent with an $S = 37$ spin ground state, although at low temperatures, the intermolecular antiferromagnetic exchange interactions cause a decrease of the χ_mT value. It is worth mentioning that, structurally, these Mn_{17} complexes are very similar to the Mn_{19} complex with a record ground-state $S = 83/2$, which has two supertetrahedra sharing a vertex,[7] and also to some Mn_{10} complexes formed by only one $Mn^{II}_4Mn^{III}_6$ supertetrahedron with the highest spin possible $S = 22$.[14,15] In this family of complexes with the $Mn^{II}_4Mn^{III}_6$ supertetrahedron, despite the very large S values, the anisotropic barriers are rather low. The origin of the anisotropy is the distorted Mn^{III} cations; the contribution of the isotropic Mn^{II} centers must be low in comparison. The analysis of the orientation of the Jahn−Teller axis in the octahedron formed by six Mn^{III} cations shows three cations with a parallel alignment of the axis; however, the other three are perpendicular. Hence, the total anisotropy of the system is relatively low.

One crucial point required to rationalize the synthesis of such systems is the knowledge of the sign and the strength of the exchange interaction constants (J) present in such systems, because they control the total spin of the molecule. From an experimental point of view, the extraction of these values using a Hamiltonian model from the measured magnetic susceptibility is straightforward only when the system is relatively simple; otherwise there are two main problems in the fitting procedure: (i) the need for too large amount of memory, when the system is very large, and (ii) the presence of many exchange coupling constants that, jointly with a simple shape of the measured susceptibility curve, make impossible to obtain a single set of fitted parameters. Theoretical methods based on density functional theory (DFT) can go beyond these limitations and calculate the exchange coupling constants from the energy of different spin distributions.[16−18] Due to the large size of the studied systems, we have employed the Siesta code[19−21] that uses a numerical basis set with generalized gradient approximation (GGA) exchange-correlation functionals, such as that proposed by Perdew, Burke, and Ernzerhof (PBE)[22] which provides good results for very large complexes. The hybrid B3LYP functional[23] together with Gaussian functions implemented in the NWChem code[24,25] has been employed to study few spin configurations, in order to corroborate the results obtained with the faster numerical code. In a previous study devoted to Mn_{10} and Mn_{19} complexes, we have employed the two theoretical approaches previously mentioned, and numerical PBE calculations always give the same sign in the interaction as the B3LYP functional with Gaussian

(11) Moushi, E. E.; Stamatatos, T. C.; Wernsdorfer, W.; Nastopoulos, V.; Christou, G.; Tasiopoulos, A. J. *Inorg. Chem.* **2009**, *48*, 5049.
(12) Nayak, S.; Lan, Y.; Clérac, R.; Hearns, N. G. R.; Wensdorfer, W.; Anson, C. E.; Powell, A. K. *Dalton Trans.* **2009**, 1901.
(13) Moushi, E. E.; Stamatatos, T. C.; Nastopoulos, V.; Christou, G.; Tasiopoulos, A. J. *Polyhedron* **2009**, 1814.
(14) Manoli, M.; Johnstone, R. D. L.; Parsons, S.; Murrie, M.; Affronte, M.; Evangelisti, M.; Brechin, E. K. *Angew. Chem., Int. Ed.* **2007**, *46*, 4456.
(15) Stamatatos, T. C.; Abboud, K. A.; Wensdorfer, W.; Christou, G. *Angew. Chem., Int. Ed.* **2006**, *45*, 4134.
(16) Ruiz, E.; Alemany, P.; Alvarez, S.; Cano, J. *J. Am. Chem. Soc.* **1997**, *119*, 1297.
(17) Ruiz, E.; Alvarez, S.; Cano, J.; Polo, V. *J. Chem. Phys.* **2005**, *123*, 164110.
(18) Ruiz, E.; Cano, J.; Alvarez, S. *Chem.—Eur. J.* **2005**, *11*, 4767.
(19) Artacho, E.; Gale, J. D.; García, A.; Junquera, J.; Martin, R. M.; Ordejón, P.; Sánchez-Portal, D.; Soler, J. M. *Siesta 2.0*; Fundación General Universidad Autonóma, de Madrid: Madrid, Spain, 2006.
(20) Artacho, E.; Sánchez-Portal, D.; Ordejón, P.; García, A.; Soler, J. M. *Phys. Stat. Sol. A* **1999**, *215*, 809.
(21) Soler, J. M.; Artacho, E.; Gale, J. D.; García, A.; Junquera, J.; Ordejón, P.; Sánchez-Portal, D. *J. Phys.: Condens. Matter* **2002**, *14*, 2745.
(22) Perdew, J.; Burke, K.; Ernzerhof, M. *Phys. Rev. Lett.* **1996**, *77*, 3865.
(23) Becke, A. D. *J. Chem. Phys.* **1993**, *98*, 5648.
(24) Kendall, R. A.; Aprà, E.; Bernholdt, D. E.; Bylaska, E. J.; Dupuis, M.; Fann, G. I.; Harrison, R. J.; Ju, J. L.; Nichols, J. A.; Nieplocha, J.; Straatsma, T. P.; Windus, T. L.; Wong, A. T. *Comput. Phys. Commun.* **2000**, *128*, 260.
(25) Aprà, E.; Windus, T. L.; Straatsma, T. P.; Bylaska, E. J.; de Jong, W.; Hirata, S.; Valiev, M.; Hackler, M.; Pollack, L.; Kowalski, K.; Harrison, R.; Dupuis, M.; Smith, D. M. A.; Nieplocha, J.; V., T.; Krishnan, M.; Auer, A. A.; Brown, E.; Cisneros, G.; Fann, G.; Fruchtl, H.; Garza, J.; Hirao, K.; Kendall, R.; Nichols, J.; Tsemekhman, K.; Wolinski, K.; Anchell, J.; Bernholdt, D.; Borowski, P.; Clark, T.; Clerc, D.; Dachsel, H.; Deegan, M.; Dyall, K.; Elwood, D.; Glendening, E.; Gutowski, M.; Hess, A.; Jaffe, J.; Johnson, B.; Ju, J.; Kobayashi, R.; Kutteh, R.; Lin, Z.; Littlefield, R.; Long, X.; Meng, B.; Nakajima, T.; Niu, S.; Rosing, M.; Sandrone, G.; Stave, M.; Taylor, H.; Thomas, G.; van Lenthe, J.; Wong, A.; Zhang, Z. *NWChem 4.5*; Pacific Northwest National Laboratory: Richland, WA, 2005.

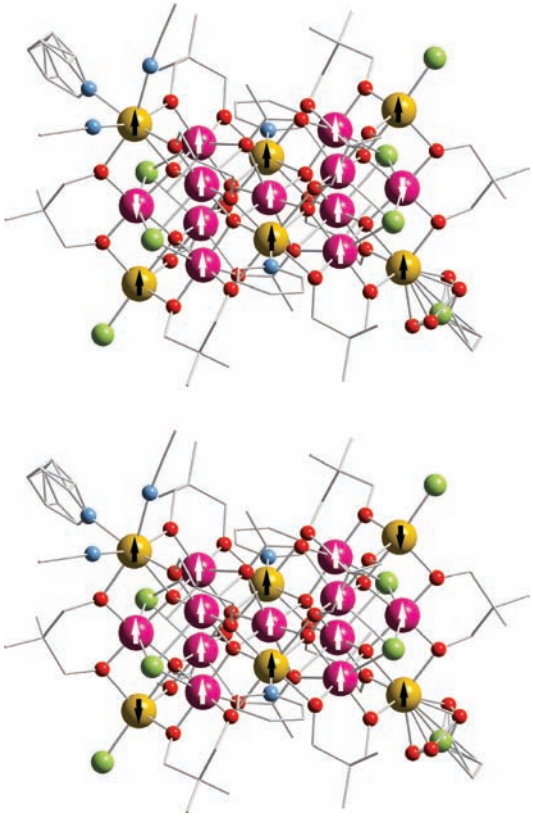

Figure 2. Scheme of two proposed spin distributions for $S = 29$ (above) and $S = 27$ (below) for complex **2**.

basis sets. Although the PBE results give slightly larger values than the hybrid functional.

Results and Discussion

Structural Analysis of the Complexes. The molecular structures of both Mn_{17} complexes are represented in Figure 1.[11,12] The structures show a common motif, as mentioned above: a Mn_{10} core that can be described as a supertetrahedron with Mn^{II} and Mn^{III} cations at vertices and edges, respectively, with two supertetrahedra sharing one edge to build up a Mn_{17} compound.

Complex **1** shows a total spin value $S = 37$, the highest possible for this compound and the second largest reported to date. This value entails a predominant ferromagnetic coupling between all manganese cations independently of their oxidation state, such as in the Mn_{19} complex.[7] The presence of some frustrated very weak antiferromagnetic interactions should also be possible. On the other hand, complex **2** shows a total spin value $S = 28 \pm 1$. Contrary to complex **1**, some of the antiferromagnetic exchange interactions should be strong enough to have inverted some spins. The authors proposed two hypothesis[12] in the original paper: (i) The spins of two Mn^{III} ions are antiparallel to all Mn^{II}'s and the remaining nine Mn^{III} ions, giving a total spin value $S = 29$. (ii) The spins of two Mn^{II} ions are antiparallel to the spins of all Mn^{III} ions and the remaining four Mn^{II} ions, pointing out a total spin value $S = 27$ (Figure 2).

Then, the question that should be answered is straightforward: where does this different behavior for complex **1** and complex **2** come from? Complex **1** shows an inversion center that makes the two supertetrahedra units perfectly symmetric, while complex **2** does not. A careful look at both structures (see Figure 1) allows one to see four main differences between them that could affect the total spin values: (i) The bridging ligands are practically identical, with the exception of those that bridge the Mn^{III} cations that are not shared by the two supertetrahedra. In complex **1**, this ligand is a μ_3-1,1,1-azide anion, while in complex **2**, it is a chloride anion. (ii) For both complexes, the two shared Mn^{II} ions are seven-coordinated (really, $5 + 2$ coordination) with a capped trigonal prism environment. For complex **1**, the rest of the Mn^{II} ions are seven-coordinated, showing a capped octahedral geometry. Meanwhile, in complex **2**, two of the four corner Mn^{II} atoms are pentacoordinated with a distorted trigonal bipyramid coordination sphere. Usually, the higher the coordination number, the longer are the metal−ligand distances. In the case of penta-coordinated Mn^{II} atoms, the metal−ligand distances are shorter (~ 0.1 Å) than in seven-coordinated Mn^{II} ions. (iii) Moreover, the coordination sphere of all Mn^{III} atoms is almost always octahedral distorted ($5 + 1$ coordination), except for two of these cations (labeled as 3 and 8 in Figure 3) in complex **1**, where they show a very long distance with an oxygen from the carboxylate bridging ligand (Mn−O ~ 2.7 Å) adopting a very distorted octahedral coordination near to square pyramidal geometry. (iv) X-ray data of complex **2** established a disordered structure for the terminal ligands of two nonshared Mn^{II} ions (see Figure 1 or 2). Obviously, this structural disorder could hinder a good extraction of J values since very few structural changes could affect dramatically the magnetic behavior of compounds.

Exchange Interactions in Mn_{17} Complexes. Once the main differences between the two compounds have been pointed out, it is possible to establish the different exchange pathways for complexes **1** and **2**. As a result of the presence of an inversion center in the former, a lower number of exchange interactions than for the latter have been considered. Hence, there are 23 different exchange pathways for complex **1** that go up to 31 for complex **2**, resulting in the following Heisenberg Hamiltonian for the former:

$$\begin{aligned}\hat{H} = & -J_1[\hat{S}_1\hat{S}_{12} + \hat{S}_1\hat{S}_{13}] - J_2[\hat{S}_2\hat{S}_{12} + \hat{S}_7\hat{S}_{13}] \\ & - J_3[\hat{S}_3\hat{S}_{13} + \hat{S}_8\hat{S}_{12}] - J_4[\hat{S}_4\hat{S}_{13} + \hat{S}_9\hat{S}_{12}] - J_5[\hat{S}_5\hat{S}_{12} + \hat{S}_{10}\hat{S}_{13}] \\ & - J_6[\hat{S}_3\hat{S}_{14} + \hat{S}_8\hat{S}_{15}] - J_7[\hat{S}_2\hat{S}_{14} + \hat{S}_7\hat{S}_{15}] - J_8[\hat{S}_4\hat{S}_{16} + \hat{S}_9\hat{S}_{17}] \\ & - J_9[\hat{S}_5\hat{S}_{16} + \hat{S}_{10}\hat{S}_{17}] - J_{10}[\hat{S}_6\hat{S}_{16} + \hat{S}_{11}\hat{S}_{17}] \\ & - J_{11}[\hat{S}_6\hat{S}_{14} + \hat{S}_{11}\hat{S}_{15}] - J_{12}[\hat{S}_1\hat{S}_3 + \hat{S}_1\hat{S}_8] \\ & - J_{13}[\hat{S}_1\hat{S}_2 + \hat{S}_1\hat{S}_7] - J_{14}[\hat{S}_1\hat{S}_4 + \hat{S}_1\hat{S}_9] - J_{15}[\hat{S}_1\hat{S}_5 + \hat{S}_1\hat{S}_{10}] \\ & - J_{16}[\hat{S}_2\hat{S}_3 + \hat{S}_7\hat{S}_8] - J_{17}[\hat{S}_4\hat{S}_5 + \hat{S}_9\hat{S}_{10}] - J_{18}[\hat{S}_4\hat{S}_6 + \hat{S}_9\hat{S}_{11}] \\ & - J_{19}[\hat{S}_5\hat{S}_6 + \hat{S}_{10}\hat{S}_{11}] - J_{20}[\hat{S}_3\hat{S}_6 + \hat{S}_8\hat{S}_{11}] \\ & - J_{21}[\hat{S}_2\hat{S}_6 + \hat{S}_7\hat{S}_{11}] - J_{22}[\hat{S}_2\hat{S}_5 + \hat{S}_7\hat{S}_{10}] \\ & - J_{23}[\hat{S}_3\hat{S}_4 + \hat{S}_8\hat{S}_9] \end{aligned} \quad (1)$$

where $\hat{S}_i$ are the local spin operators of each paramagnetic center (Figure 3). For complex **2**, J_1-J_3, J_8-J_{11}, and J_{23} are split up into two different coupling constants.

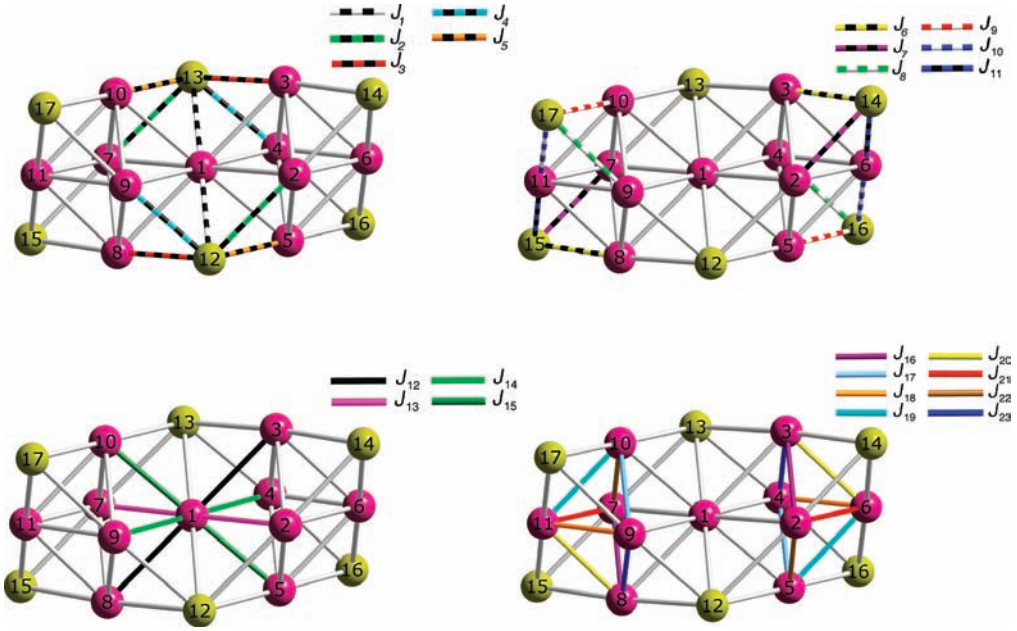

Figure 3. Exchange pathways employed to calculate the J values for complex **1**. The models above describe the $Mn^{II}-Mn^{III}$ interactions[12] of the two shared Mn^{II} cations, J_1-J_5, and the nonshared Mn^{II} atoms, J_6-J_{11}. The models below describe $Mn^{III}-Mn^{III}$ interactions of the central Mn^{III} ion, $J_{12}-J_{15}$, and the rest of the Mn^{III} cations, $J_{16}-J_{23}$, from left to right.

In a previous theoretical study,[26] some related compounds were studied: a Mn_{10} supertetrahedron[14,15] and a Mn_{19} compound where two supertetrahedra units were sharing one vertex.[7] In these cases, the compounds were highly symmetric, and a low number of J values were enough to describe the different exchange pathways. However, in this work, it was necessary to use a very large number of exchange pathways because of the complexity of the system.

The calculated J values for the two complexes are reported in Table 1. All interactions are relatively weak, but whereas $Mn^{III}-Mn^{III}$ interactions are always ferromagnetic for both molecules, the J values related to the $Mn^{II}-Mn^{III}$ interactions can be positive or (very weakly) negative, in agreement with the reported DFT values.[27,28] J values are put into two general groups: J_1-J_{11} values represent $Mn^{II}-Mn^{III}$ interactions, and $J_{12}-J_{23}$ values symbolize $Mn^{III}-Mn^{III}$ interactions. From the results of the calculated exchange interaction of $Mn^{II}-Mn^{III}$ interactions, some of these trends are as follows:

(i) J_1 is the only exchange pathway that has the same bridging ligands, two μ_4-oxo units, and represents the interaction along the shared edge of the two supertetrahedra. This value is weak and has a different sign depending on the compound: whereas in **1** it has a positive value, in **2** it has been split into two different exchange pathways because the difference in the two Mn−O−Mn angle values is enough to cause a different behavior, a weak ferro- and a very weak antiferromagnetic coupling.

(ii) J_2-J_{11} exchange pathways show two common bridging ligands: a μ_4-oxo and a μ_2-propanediol-κ^2,O,O for **1** and 2,2-dimethyl-1,3-propanediol for **2**. In general, we can indicate that complex **2** has stronger ferromagnetic couplings than **1**. The analysis of the geometries of the exchange pathways reveals that the Mn−X−Mn angles are smaller for complex **2**, in agreement with the usual recipe that smaller angles are close to the orthogonality of the "magnetic orbitals", resulting in stronger ferromagnetic couplings. Also, the presence of the heptacoordinated corner Mn^{II} cations in complex **1** is an important fact, while in complex **2** only one cation shows this coordination (label 17 in Figure 3), and three of them are pentacoordinated. Thus, when the split J values due to low symmetry complex **2** are analyzed, this heptacoordinated Mn^{II} cation is involved in the weaker ferromagnetic couplings (J_8-J_{10}), similar to those of complex **1**, also with a heptacoordinated cation. However, the larger ferromagnetic J_8-J_{10} values correspond to the nonequivalent pentacoordinated Mn^{II} cation (label 16 in Figure 3).

On the other hand, $Mn^{III}-Mn^{III}$ interactions could be divided into two groups (see Figure 3) depending on whether the central Mn^{III} cation ($J_{12}-J_{15}$) is involved or not ($J_{16}-J_{23}$). If we employ the bridging ligands as a criterion for the classification, there are also two groups, the first one ($J_{12}-J_{17}$) with μ_4-oxo and μ-acetato-κ^2,O,O as bridging ligands. The second group ($J_{18}-J_{23}$) shows a μ_4-oxo and a μ_3-X_3 entity, where X_3 could be an azide (**1**) or a chloride (**2**) anion. For both complexes, again in most of the cases, the decrease of the Mn−X−Mn angle is related to an increase of the ferromagnetic coupling, as previously found for Mn_{10} and Mn_{19} complexes.[26]

The second group of interactions, $J_{18}-J_{23}$ showing azide or chloride anions, has been pointed out as a possible explanation for the different total spin value, S,

(26) Ruiz, E.; Cauchy, T.; Cano, J.; Costa, R.; Tercero, J.; Alvarez, S. *J. Am. Chem. Soc.* **2008**, *130*, 7420.
(27) Cremades, E.; Cauchy, T.; Cano, J.; Ruiz, E. *Dalton Trans.* **2009**, 5873.
(28) Rajaraman, G.; Mugurescu, M.; Sañudo, C. E.; Soler, M.; Wernsdorfer, W.; Helliwell, M.; Muryn, C.; Raftery, J.; Teat, S. J.; Christou, G.; Brechin, E. K. *J. Am. Chem. Soc.* **2004**, *126*, 15445.

Table 1. Calculated Exchange Coupling Constants Using Numerical Calculations with the PBE Functional (in cm^{-1}) for the Two Mn_{17} Complexes Together with the Corresponding Bridging Ligands and Geometrical Parameters (in Å and deg)

	bridging ligands		Mn···Mn		Mn−X−Mn		J_{calc}	
	1	**2**	**1**	**2**	**1**	**2**	**1**	**2**
				$Mn^{II}-Mn^{III}$/shared Mn^{II} cations				
J_1	2(μ_4-O)		3.216	3.202 3.195	99.8/100.0	99.6/99.7 98.5/100.0	+3.6	−0.4 +8.3
J_2	(μ_4-O) (μ_2-diol)		3.365	3.442 3.382	105.7/106.4	100.6/109.5 101.1/107.3	+7.5	+7.8 +11.2
J_3	(μ_4-O) (μ_2-diol)		3.361	3.380 3.351	104.9/105.8	102.1/106.8 102.0/106.2	+13.5	+13.4 +25.3
J_4	(μ_4-O) (μ_2-diol)		3.214	3.226	100.0/105.1	99.8/104.6	+5.8	+7.9
J_5	(μ_4-O) (μ_2-diol)		3.208	3.215	98.5/106.3	98.8/104.4	−2.8	−4.1
				$Mn^{II}-Mn^{III}$/nonshared Mn^{II} cations				
J_6	(μ_4-O) (μ_2-diol)		3.317	3.172	102.7/107.7	100.2/103.6	+7.5	+27.5
J_7	(μ_4-O) (μ_2-diol)		3.312	3.188	102.2/108.1	101.2/103.8	−0.1	+19.2
J_8	(μ_4-O) (μ_2-diol)		3.275	3.278 3.197	102.8/105.8	101.3/106.6 100.6/104.7	+1.7	+4.5 +17.1
J_9	(μ_4-O) (μ_2-diol)		3.246	3.305 3.227	102.4/106.9	102.6/106.3 102.3/104.5	+5.6	+8.3 +30.0
J_{10}	(μ_4-O) (μ_2-diol)		3.245	3.258 3.159	100.9/105.7	100.4/104.8 99.4/102.4	+6.4	+3.4 +15.6
J_{11}	(μ_4-O) (μ_2-diol)		3.236	3.121 3.108	100.3/106.1	98.0/102.1 97.9/101.1	+3.9	+10.1 +11.4
				$Mn^{III}-Mn^{III}$/central Mn^{III} cation				
J_{12}	(μ_4-O)	(μ_4-O) (μ_5-O_2CMe)	3.432	3.430	125.5	124.6	+2.5	+2.9
J_{13}	(μ_4-O) (μ_4-O_2CMe)	(μ_4-O) (μ_5-O_2CMe)	3.411	3.436	126.0	124.2	+3.1	+5.3
J_{14}	(μ_4-O) (μ_4-O_2CMe)	(μ_4-O) (μ_5-O_2CMe)	3.229	3.242	87.3/114.4	88.2/112.8	+16.4	+18.5
J_{15}	(μ_4-O) (μ_4-O_2CMe)	(μ_4-O) (μ_5-O_2CMe)	3.209	3.269	87.0/113.5	88.6/113.4	+16.5	+18.6
				$Mn^{III}-Mn^{III}$/noncentral Mn^{III} cation				
J_{16}	(μ_4-O)	(μ_4-O) (μ_5-O_2CMe)	3.341	3.292	81.0/121.6	85.0/118.4	+8.2	+10.7
J_{17}	(μ_4-O)(μ_4-O_2CMe)	(μ_4-O) (μ_5-O_2CMe)	3.232	3.272	83.6/116.1	85.2/117.4	+19.6	+20.7
J_{18}	(μ_4-O)(μ_3-N_3)	(μ_4-O)(μ_3-Cl)	3.255	3.236	85.3/115.1	75.0/115.4	+20.9	+21.9
J_{19}	(μ_4-O)(μ_3-N_3)	(μ_4-O)(μ_3-Cl)	3.250	3.249 3.242	86.3/116.2	74.8/116.7 74.4/115.9	+25.1	+20.7 +26.8
J_{20}	(μ_4-O)(μ_3-N_3)	(μ_4-O)(μ_3-Cl)	3.164	3.246	84.0/113.6	75.4/115.6	+12.4	+6.2
J_{21}	(μ_4-O)(μ_3-N_3)	(μ_4-O)(μ_3-Cl)	3.150	3.271	83.4/112.4	75.3/117.4	+19.9	+22.4
J_{22}	(μ_4-O)(μ_3-N_3)	(μ_4-O)(μ_3-Cl)	3.136	3.188	84.4/108.7	73.6/109.0	+16.6	+10.9
J_{23}	(μ_4-O)(μ_3-N_3)	(μ_4-O)(μ_3-Cl)	3.109	3.194	84.0/107.3	75.0/109.5	+13.1	+8.9

determined experimentally. It is well-known that the use of the N_3^- group when it bridges in the end-on (1,1) coordination mode gives ferromagnetic interactions,[29] while this is not always true when the bridging ligand is a chloride anion.[30−44] However, the long Mn−N and Mn−Cl distances adopted in these two studied complexes caused by the Jahn−Teller effect seem to diminish the role of the nature of ligands, resulting in ferromagnetic interactions,[45,46] as has been previously shown for the Mn_{10} complexes.[26]

In summary, the exchange coupling constants obtained from calculations, beyond the coordination environment of the manganese atoms and the type of bridging ligands, almost always show positive ferromagnetic values (see Figure 4), ruling out the $S = 29$ and $S = 27$ hypotheses for complex **2**. Hence, the calculated exchange coupling

(29) Escuer, A.; Aromi, G. *Eur. J. Inorg. Chem.* **2006**, 4721.
(30) Aromi, G.; Claude, J.-P.; Knapp, M. J.; Huffman, J. C.; Hendrickson, D. N.; Christou, G. *J. Am. Chem. Soc.* **1998**, *120*, 2977.
(31) Aromi, G.; Knapp, M. J.; Claude, J.-P.; Huffman, J. C.; Hendrickson, D. N.; Christou, G. *J. Am. Chem. Soc.* **1999**, *121*, 5489.
(32) Boskovic, C.; Bircher, R.; Tregenna-Piggott, P. L. W.; Gudel, H. U.; Paulsen, C.; Wernsdorfer, W.; Barra, A.-L.; Khatsko, E.; Neels, A.; Stoeckli-Evans, H. *J. Am. Chem. Soc.* **2003**, *125*, 14046.
(33) Boskovic, C.; Rusanov, E.; Stoeckli-Evans, H.; Güdel, H. U. *Inorg. Chem. Commun.* **2002**, *5*, 881.
(34) Bossek, U.; Nuhlen, D.; Bill, E.; Glaser, T.; Krebs, C.; Weyhermuller, T.; Wieghardt, K.; Lengen, M.; Trautwein, A. X. *Inorg. Chem.* **1997**, *36*, 2834.
(35) Diril, H.; Chang, H. R.; Zhang, X.; Larsen, S. K.; Potenza, J. A.; Pierpont, C. G.; Schugar, H. J.; Isied, S. S.; Hendrickson, D. N. *J. Am. Chem. Soc.* **1987**, *109*, 6207.
(36) Fu, Y.; Li, Q.; Zhou, Z.; Dai, W.; Wang, D.; Mak, T. C. W.; Hu, W.; Tang, W. *Chem. Commun.* **1996**, 1549.
(37) Hendrickson, D. N.; Christou, G.; Schmitt, E. A.; Libby, E.; Bashkin, J. S.; Wang, S.; Tsai, H. L.; Vincent, J. B.; Boyd, P. D. W. *J. Am. Chem. Soc.* **1992**, *114*, 2455.
(38) Qi, C.-M.; Sun, X.-X.; Gao, S.; Ma, S.-L.; Yuan, D.-Q.; Fan, C.-H.; Huang, H.-B.; Zhu, W.-X. *Eur. J. Inorg. Chem.* **2007**, 3663.
(39) Romero, I.; Collomb, M.-N.; Deronzier, A.; Llobet, A.; Perret, E.; Pècaut, J.; Pape, L. L.; Latour, J.-M. *Eur. J. Inorg. Chem.* **2001**, 69.
(40) Shin, B.-K.; Kim, Y.; Kim, M.; Han, J. *Polyhedron* **2007**, *26*, 4557.
(41) van Albada, G. A.; Mohamadou, A.; Driessen, W. L.; de Gelder, R.; Tanase, S.; Reedijk, J. *Polyhedron* **2004**, *23*, 2387.
(42) Wang, S.; Tsai, H. L.; Libby, E.; Folting, K.; Streib, W. E.; Hendrickson, D. N.; Christou, G. *Inorg. Chem.* **1996**, *35*, 7578.
(43) Wemple, M. W.; Tsai, H. L.; Folting, K.; Hendrickson, D. N.; Christou, G. *Inorg. Chem.* **1993**, *32*, 2025.
(44) Wu, J.-Z.; Bouwman, E.; Mills, A. M.; Spek, A. L.; Reedijk, J. *Inorg. Chim. Acta* **2004**, *357*, 2694.
(45) Aubin, S. M. J.; Wemple, M. W.; Adams, D. M.; Tsai, H.-L.; Christou, G.; Hendrickson, D. N. *J. Am. Chem. Soc.* **1996**, *118*, 7746.
(46) Wemple, M. W.; Adams, D. M.; Hagen, K. S.; Folting, K.; Hendrickson, D. N.; Christou, G. *J. Chem. Soc., Chem. Commun.* **1995**, 1591.

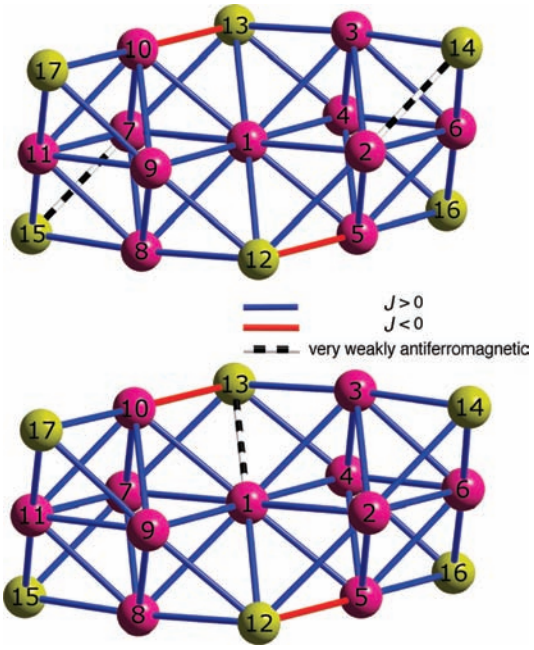

Figure 4. Schematic representation of the calculated J values for complexes **1** (above) and **2** (below). Ferromagnetic and antiferromagnetic interactions are represented as blue and red cylinders, respectively, while black and white rendered cylinders are equivalent to those exchange interactions that are very weakly antiferromagnetic.

constants point out the same total spin value for both complexes, $S = 37$, as the energy of the high spin distribution, the one where all the spins are parallel, is the lowest for all of the calculated distributions (see Computational Details). It is worth noting the antiferromagnetic couplings found for the J_5 interaction in both complexes, especially, taking into account that this interaction shows the shortest Mn···Mn distance (and consequently small Mn−X−Mn angles) of the J_2−J_5 similar interactions. Due to the overall ferromagnetic coupling, such antiferromagnetic J_5 interactions will remain frustrated, and the highest possible spin $S = 37$ should be found in both complexes.

Comparison with Mn_{19} Complexes. Previously, we have studied one Mn_{10} and one Mn_{19} complex (**3**) that, as has been said before, showed the same structural motif, the $Mn^{II}_4Mn^{III}_6$ supertetrahedron, as the two Mn_{17} compounds.[26] The theoretical study, as well as the experimental results, concluded that the total spin value for both complexes is the highest possible, $S = 22$ and 83/2, respectively. However, a new Mn_{19} complex (**4**) has been recently synthesized showing an $S = 73/2$,[47] although its molecular structure is very similar to that of the first Mn_{19} compound (see Figure 5). This total spin value agrees with a most stable spin distribution corresponding to the spin inversion of the central shared Mn^{II} cation. The geometrical parameters around the central Mn^{II} atom are slightly different for complexes **3** and **4** (Table 2); hence, the authors propose that the longer Mn^{II}−Mn^{III} separation for the latter could justify the different magnetic behavior, although the antiferromagnetic coupling should be comparatively weak. In order to corroborate

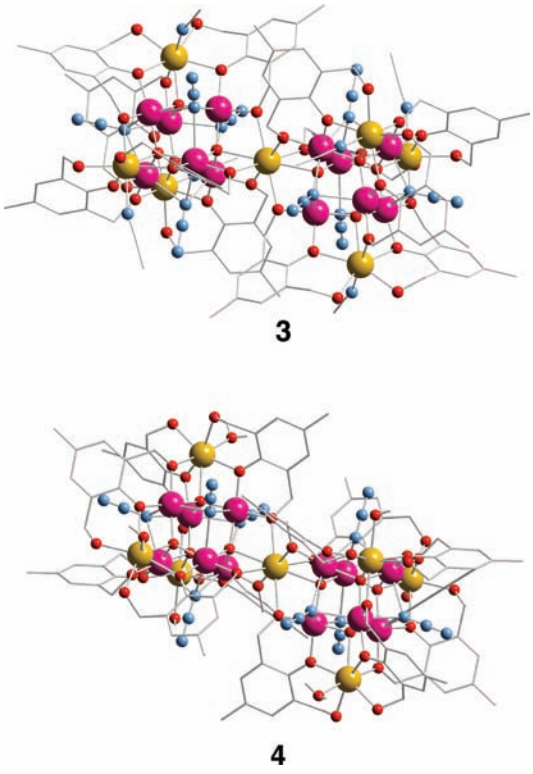

Figure 5. Molecular structure of Mn_{19} complexes. $[Mn^{II}_7Mn^{III}_{12}(\mu_4\text{-}O)_8(\mu_3\text{-}N_3)_8(HL)_{12}(MeCN)_6]^{2+}$ (**3**) and $[Mn^{II}_7Mn^{III}_{12}(\mu_4\text{-}O)_8(\mu_3\text{-}N_3)_8(HL)_{12}(OH)_2(H_2O)_4]$ (**4**) (H_3L = 2,6-bis(hydroxymethyl)-4-methyl-phenol).

such assumptions and due to the similarity of the magnetic properties of complexes **1** and **2**, we performed calculations for complex **4**, a high spin distribution ($S = 83/2$) and the spin distribution with the central Mn^{II} atoms with inverted spin ($S = 73/2$). We determined that the high spin distribution is the most stable one, contrary to the experimental evidence. It is possible to estimate an average J value of the interaction of the central Mn^{II} ion with the surrounding Mn^{III} atoms, using the energies of the calculated $S = 73/2$ and $S = 83/2$ spin distributions, giving $J = +4\ cm^{-1}$ (Table 2).

In order to verify the accuracy of the numerical calculations using the PBE functional, which usually gives good results, the computationally more expensive B3LYP functional combined with Gaussian functions has been employed (see the Computational Details), which gives excellent results for these kinds of complexes, taking into account that only two spin distributions must be considered to check the ground state of these Mn_{19} complexes. The computed J values are ferromagnetic and similar for the two complexes (see Table 2). The calculated energies of the two spin distributions with the B3LYP functional follow the same trend as that calculated with the PBE functional, pointing out a total spin value $S = 83/2$. To see how the distance of the central Mn^{II} cation to the neighboring Mn^{III} atoms could affect the total spin value of this Mn_{19} complex, the cluster has been distorted, increasing the Mn^{II}···Mn^{III} distance (complex **4***, Table 2). The tendency observed is an increase of the ferromagnetic behavior with the increase of the metal−metal distance that cannot explain the different total spin values for such compounds. These results are in agreement with those obtained previously by us to explain the ferromagnetic

(47) Ge, C.-H.; Ni, Z.-H.; Liu, C.-M.; Cui, A.-L.; Zhang, D.-Q.; Kou, H.-Z. *Inorg. Chem. Commun.* **2008**, *11*, 675.

Table 2. Calculated Average Exchange Coupling Constant (in cm^{-1}) Using the B3LYP Functional (PBE values in parentheses) for the Interaction of the Central Mn^{II} Atom with the Surrounding Mn^{III} Cations of Mn_{19} Complexes (**3** and **4**) and the Distorted **4*** Complex Together with the Corresponding Geometrical Parameters (in Å and deg)

complex	bridging ligands	$Mn^{II}\cdots Mn^{III}$	Mn−O[a]	Mn−O−Mn	J_{calc}
3	(μ_4-O) (μ-OR)	3.436	*2.335, 2.509* 1.854, 1.891	101.8, 109.3	+1.8 (+3.6)
4	(μ_4-O) (μ-OR)	3.457	*2.397, 2.515* 1.855, 1.899	102.2	+2.0 (+4.0)
4*	(μ_4-O) (μ-OR)	3.600	*2.478, 2.684* 1.855, 1.899	108.1	+2.8 (+6.0)

[a] Values in italics correspond to the Mn^{II} cations.

coupling in the Mn_{19} complex with $S = 83/2$ due to the large coordination number of the Mn^{II} cations that results in long bond distances.

Structural Modifications in Mn_{17} Complexes. Focusing again on the Mn_{17} complexes, we have performed a similar study to that presented previously for the Mn_{19} complexes. The high spin distribution and different spin distributions that could lead to values close to $S = 28$ have been recalculated with the B3LYP functional. We compared the total energies corresponding to the inversion of {Mn12, Mn13} and {Mn16, Mn17} (see Figure 4), because they have $S = 27$, with the high spin solution $S = 37$. The second $S = 27$ distribution is the more stable, but still around 250 cm^{-1} above that of the high spin state. Again, the B3LYP and PBE functionals agreed that the highest spin distribution is the most stable for both Mn_{17} complexes.

As pointed previously, it is possible to suggest an alternative origin of the lower S value of complex **2** that could be due to the problems of having the right structure to perform the calculations caused by disorder found in the X-ray structure, especially in the Mn^{II} atoms placed on the corners of the molecule (see Figure 1 or 2). Hence, to understand how the geometrical parameters of the corner Mn^{II} ions could modulate the strength (and the sign) of the exchange coupling constants, the Mn^{II} ion has been displaced with respect to the μ_3-oxo group that is bridging it with the neighboring Mn^{III} cations (Figure 6). The increase of 0.2 Å in the Mn−O distance reduces the J value from +20.9 (average of the second value of J_8, J_9, and J_{10} for **2** in Table 1) to +12.7 cm^{-1} using numerical PBE calculations, while the decrease of 0.1 Å in such a Mn−O distance results in a value of +23.1 cm^{-1}. Using the same procedure for the terminal Mn^{II} cation coordinated to the pyridine, the J value remains practically unchanged, from a value of +5.4 cm^{-1} for the nondistorted structure to a J value +5.0 cm^{-1}, increasing by 0.1 Å the Mn−O distance, and a value of +5.6 cm^{-1}, shortening by 0.1 Å the same distance. Thus, these dependences for the external Mn^{II} cations are the opposite of that found for the central Mn^{II} cation in the Mn_{19} complex (see Table 2). As a conclusion, it is possible to indicate that there is not clear evidence about the existence of antiferromagnetic interactions that can give a reduction of the highest-possible spin value for these kinds of complexes, but the presence of disorder in the X-ray structure in complex **2** could avoid an accurate estimation of the J values.

Concluding Remarks

The analysis of the calculated J values of two Mn_{17} complexes, together with a Mn_{19} complex, agrees with previous calculations of Mn_{10} and Mn_{19} complexes[11,12] based on the $Mn^{II}_4Mn^{III}_6$ supertetrahedron structure, pointing out a predominance of the ferromagnetic interactions between the manganese centers. Therefore, they exhibit the maximum possible total spin value. However, one of the two studied Mn_{17} complexes and another reported Mn_{19} compound show experimental evidence of smaller S values that obviously do not match with these computational results. The study was carried out using numerical calculations with a PBE functional, but also some B3LYP calculations were performed to reach a greater accuracy and to verify the results. The problem of the estimation of the J values for the Mn_{17} complex with a smaller S value could be related to the disorder of the X-ray structure. Thus, the lack of a good crystal structure could help to avoid a proper calculation of the exchange coupling constants for this complex.

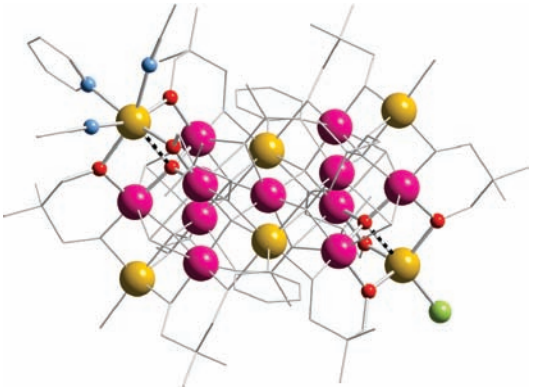

Figure 6. Description of the distortion of complex **2** employed to check the dependence of the exchange coupling constant with modification in the coordination of the nonshared Mn^{II} atoms that have been moved along the direction of the Mn−O bond, represented with a black and white rendered cylinder.

Computational Details

The spin Hamiltonian for a general polynuclear complex is indicated in eq 1a:

$$\hat{H} = -\sum_{i>j} J_{ij}\hat{S}_i\hat{S}_j + D\left(\hat{S}_z^2 - \frac{1}{3}\hat{S}^2\right) + E(\hat{S}_x^2 - \hat{S}_y^2) \quad (1a)$$

where $\hat{S}_i$ and $\hat{S}_j$ are the spin operators of the paramagnetic centers i and j and $\hat{S}$ and $\hat{S}_z$ are the total spin operators of the molecule and its axial component, respectively. The J_{ij} values are the coupling constants for the different exchange pathways between all the paramagnetic centers of the molecule, while D and E are the axial and rhombic components of the anisotropy, respectively.[48] For the calculation of zero-field

(48) Kortus, J.; Pederson, M. R.; Baruah, T.; Bernstein, N.; Hellberg, C. S. *Polyhedron* **2003**, *22*, 1871.

splitting D and E parameters, it is indispensable to include spin−orbit coupling effects in the electronic structure calculations. However, in this work, we will focus only on the calculation of exchange coupling values.

A more detailed description of the procedure to obtain the exchange coupling constants can be found in previous publications.[49−51] Basically, we need to calculate at least the energy of $n + 1$ spin distributions if we have a system with n different exchange coupling constants. These values will allow us to build up a system of n equations where the J values are the unknowns. If more energy values are calculated, a fitting procedure is required to extract the J values. Therefore, 26 calculations were performed for complex **1**: a high-spin solution ($S = 37$); two $S = 32$ configurations with negative spin at {Mn16} and {Mn17}; 16 $S = 29$ configurations with negative spin at {Mn2, Mn7}, {Mn4, Mn9}, {Mn3, Mn8}, {Mn5, Mn10}, {Mn6, Mn11}, {Mn1, Mn2}, {Mn1, Mn4}, {Mn4, Mn10}, {Mn9, Mn10}, {Mn2, Mn5}, {Mn2, Mn6}, {Mn4, Mn6}, {Mn5, Mn6}, {Mn3, Mn4}, {Mn1, Mn3}, and {Mn2, Mn4}; five $S = 28$ configurations with negative spin at {Mn10, Mn17}, {Mn1, Mn12}, {Mn8, Mn15}, {Mn6, Mn14}, and {Mn5, Mn16}; and two $S = 27$ configurations with negative spin at {Mn12, Mn13} and {Mn14, Mn15}. The same configurations plus three $S = 29$ configurations with negative spin at {Mn4, Mn5}, {Mn1, Mn5}, and {Mn1, Mn7} and four $S = 28$ configurations with negative spin at {Mn6, Mn16}, {Mn11, Mn17}, {Mn1, Mn13}, and {Mn3, Mn14} have been used for complex **2**.

The computer code employed for all calculations was the program SIESTA (Spanish Initiative for Electronic Simulations with Thousands of Atoms).[19−21,52] This code has been developed and designed for efficient calculations in large and low symmetry systems. We have employed the generalized-gradient functional proposed by Perdew, Burke, and Erzernhof.[22] Only valence electrons are included in the calculations, with the core being replaced by norm-conserving scalar relativistic pseudopotentials factorized in the Kleinman−Bylander form.[53] The pseudopotentials are generated according to the procedure of Trouiller and Martins.[54] The cutoff radii were 1.14 Å for oxygen, hydrogen, and nitrogen atoms and 1.25 Å for carbon atoms. For the Mn atoms, we have employed a pseudopotential including the 3s and 3p orbitals in the basis set that we have previously tested to give accurate J values.[55] We also have employed a numerical basis set of triple-ζ quality with polarization functions for the manganese atoms and a double-ζ one with polarization functions for the main group elements.[21] There are two parameters that control the accuracy of the numerical calculation: (i) since the wave function vanishes at the chosen confinement radius r_c, whose value is different for each atomic orbital, the energy radii of different orbitals are determined by a single parameter, *the energy shift*, which is the energy increase of the atomic eigenstate due to the confinement, and (ii) the integrals of the self-consistent terms are obtained with the help of a regular real space grid in which the electron density is projected. The grid spacing is determined by the *maximum kinetic energy* of the plane waves that can be represented in that grid. Previously, we have studied the influence of these two parameters in the calculated J value. Thus, the values of 50 meV for the energy shift and 250 Ry for mesh cutoff provide a good compromise between accuracy and computer time to estimate exchange coupling constants.[55]

Calculations with the B3LYP functional[23] were performed with the NWChem code[24,25] using a guess function generated with the Jaguar 7.5 code.[56] The triple-ζ all electron Gaussian basis set proposed by Schaefer et al. was employed for all atoms.[57]

Acknowledgment. We thank the Spanish Government (CTQ2008-06670-C02-01) and Generalitat de Catalunya (Grant 2009SGR-1459) for financial support. The authors thankfully acknowledge the computer resources, technical expertise, and assistance provided by the Barcelona Supercomputer Center. E.C. thanks *Ministerio de Ciencia e Innovación* for a predoctoral fellowship (ref BES-2009-017369).

(49) Ruiz, E.; Rodríguez-Fortea, A.; Tercero, J.; Cauchy, T. *J. Chem. Phys.* **2005**, *123*, 074102.
(50) Ruiz, E. *Struct. Bonding* (*Berlin*) **2004**, *113*, 71.
(51) Ruiz, E.; Rodríguez-Fortea, A.; Cano, J.; Alvarez, S.; Alemany, P. *J. Comput. Chem.* **2003**, *24*, 982.
(52) Sánchez-Portal, D.; Ordejón, P.; Artacho, E.; Soler, J. M. *Int. J. Quantum Chem.* **1997**, *65*, 453.
(53) Kleinman, L.; Bylander, D. M. *Phys. Rev. Lett.* **1982**, *48*, 1425.
(54) Trouiller, N.; Martins, J. L. *Phys. Rev. B* **1991**, *43*, 1993.
(55) Ruiz, E.; Rodríguez-Fortea, A.; Tercero, J.; Cauchy, T.; Massobrio, C. *J. Chem. Phys.* **2005**, *123*, 074102.
(56) *Jaguar 7.5*; Schrödinger, Inc.: New York, 2009.
(57) Schaefer, A.; Huber, C.; Ahlrichs, R. *J. Chem. Phys.* **1994**, *100*, 5829.